

INVESTIGATING THE THERMOPHYSICAL PROPERTIES OF THE ICE-SNOW INTERFACE
PART II: THERMAL CONTACT RESISTANCE

Kevin Hammonds^{1*} and Ian Baker¹

¹Thayer School of Engineering at Dartmouth College, Hanover, NH, USA

ABSTRACT: As it turns out, spending many an extra cold and blustery minute trying to get those last few temperature readings to complete a textbook perfect “every-ten-centimeter” temperature profile in your snowpit may not be all that helpful, and if anything, can even be misleading. As first presented at ISSW 2014, we showed that the presence of an “ice lens” within a snowpack can cause sub-millimeter scale temperature gradients to be much larger than the “every-ten-centimeter” temperature gradient that is most commonly recorded. This occurs because such icy layers can act as a thermal discontinuity to an otherwise thermodynamically homogeneous snowpack. In order to develop a more intuitive understanding of the physical mechanisms and processes responsible for this observation and how it may also be affecting kinetic snow metamorphism at the ice-snow interface, we have since performed a more detailed and quantitative analysis of the in situ micro-thermocouple data originally presented at ISSW 2014. In this detailed analysis, we suggest and believe that our findings show, via a one-dimensional model for energy balance, that this large temperature gradient is primarily caused by the limited number of contact points that exist between the porous snow matrix and the solid layer of ice at the interface, a phenomenon known as *thermal contact resistance*. Until recently, it has been thought for many porous materials that thermal contact resistance was adequately accounted for in calculations of the effective thermal conductivity, but we contend that these two modes of heat transport should be accounted for individually.

KEYWORDS: ice lens, temperature gradient, effective thermal conductivity, thermal contact resistance, kinetic snow metamorphism

1. INTRODUCTION

Over the last several decades, understanding the thermophysical properties of seasonal snowpacks has been the focus of many field, laboratory, and modeling studies (Adams & Brown 1990, Colbeck 1991, Colbeck & Jamieson 2001, Greene 2007, Riche & Schneebeli 2013, and others). Presumably, much of this work has been motivated by the inherently dynamic characteristics of natural snowpacks, such that their thermophysical properties can be highly variable in space and time. Developing an adequate knowledge of these properties is dramatically important to many fields within the cryospheric sciences, including avalanche forecasting. At present, some of the most recent of these studies have demonstrated success with making observations or predictions of the evolution of dry snow via in situ laboratory observations (Riche & Schneebeli 2013), X-ray computed micro-tomography (Flin & Brzoska 2008, Pinzer et al. 2012), scanning electron microscopy

(Chen and Baker 2010), or three-dimensional modeling (Calonne et al. 2014). But although highly sophisticated in their approach, none of these more recent studies have begun to account for the more complex and inhomogeneous nature of natural snowpacks, such as those with inherent thermal discontinuities consisting of icy layers or crusts. Presented in this paper are some of the more pertinent findings for avalanche research stemming from a recent two-part study, first presented at ISSW 2014 and later published in Cold Regions Science and Technology (see Hammonds et al. 2015 & Hammonds & Baker 2016), that attempt to unravel some of these complexities.

2. BACKGROUND

2.1 *Previous Work*

In Part I of this study, we showed via in situ temperature measurements that a temperature gradient much larger than the imposed bulk temperature gradient can exist near the ice-snow interface in laboratory prepared specimens of artificially created ice lenses and naturally collected snow grains. After placing these ice-snow specimens under a controlled temperature gradient, we also showed via in situ X-ray micro-computed to-

* *Corresponding author address:*

Kevin Hammonds, Thayer School of Engineering at Dartmouth College, Hanover, NH 03755; tel: 603-646-6511; email: kevin.d.hammonds.th@dartmouth.edu

mography (μ -CT) and post-experiment scanning electron microscopy (SEM) that while new ice crystal growth was occurring from deposition upon the bottom (warmer) side of the ice lens, sublimation was occurring from the top (cooler) surface. In our μ -CT analysis, we found that the porosity was generally higher near the ice-snow interface than in the bulk and that the connectivity density increased at a much faster rate below the ice lens than above. We speculated in Part I that this difference in porosity was a likely contributor to the large temperature gradients observed near the ice-snow interface, but we did not attempt to quantify this effect. Also in Part I, we suggested that the diffusion of water vapor and subsequent latent heat flux may be acting to either enhance or diminish these large temperature gradients, but again could only speculate about the proportional contributions of the conductive vs. the latent heat flux. For reference, an example of a laboratory-prepared ice-snow specimen is shown in Fig. 1, while a phenomenological model of this specimen showing the expected nature of the heat flux and water vapor flux is shown in Fig. 2.



Fig. 1: Ice-snow sample with a 2 mm thick ice lens placed between natural snow with a grain size of 2.5-3 mm. Adapted from Hammonds et al. 2015 with permission from Elsevier and Cold Regions Science and Technology.

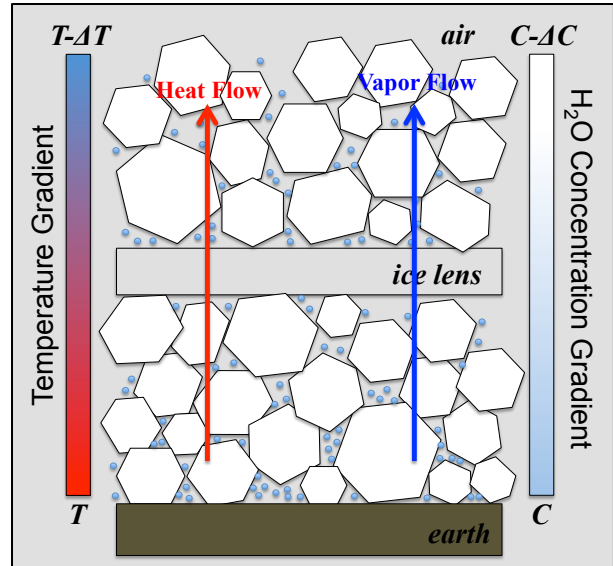


Fig. 2: Phenomenological representation of how an ice lens may affect the thermophysical properties of an ice-snow interface.

When examining Fig. 2, it becomes apparent that due to the presence of the ice lens, both the one-dimensional heat flux and water vapor flux that may be expected in a more uniform snowpack will be altered, as the ice lens acts as a physical barrier to the flow of water vapor and a thermal discontinuity to conductive heat flow. Developing a better understanding of these mechanisms and how they may contribute to mechanical instabilities in a snowpack was essentially the motivation behind this research.

Although never before directly measured, many have suggested in the past (Colbeck 1991, Colbeck & Jamieson 2001, Greene 2007, and others) that super-temperature gradients were likely to exist near such ice-snow interfaces and that enhancements in kinetic snow metamorphism could result. As a pertinent and memorable example of such a scenario, large and widespread avalanche cycles associated with the Martin Luther King (MLK) rain crust in 2011 (see TAR Vol. 30 No. 3) were more than likely the result of such enhancements in kinetic snow metamorphism occurring near an ice-snow interface. To test experimentally for the existence of such a super-temperature gradient near our ice-snow interfaces, an array of micro-thermocouples were created and placed within 1 mm above and below the ice-snow interface, while the entire specimen was held under a constant temperature gradient of $-100^{\circ}\text{C m}^{-1}$. Results from this experiment are shown in Fig. 3, where it can be observed that a super-temperature gradient was indeed found to exist in these regions.

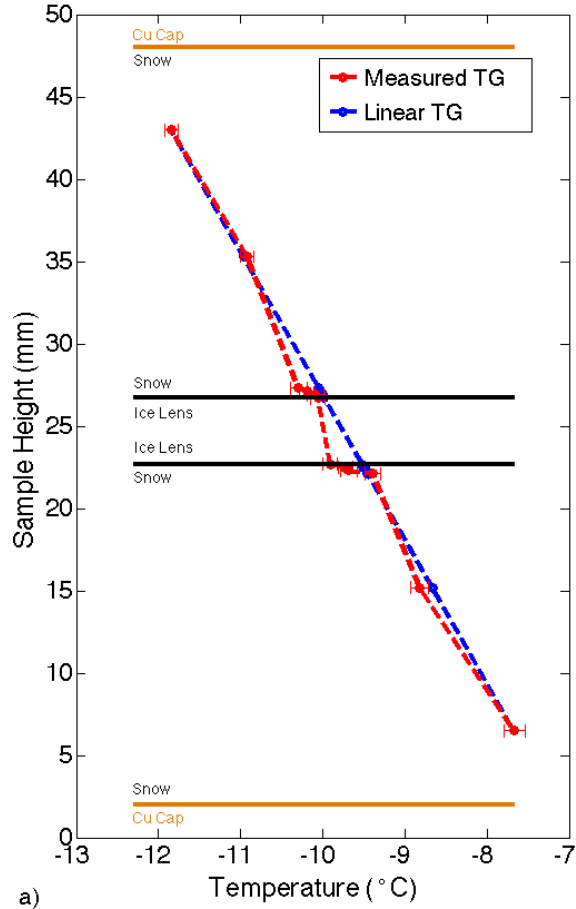


Fig. 3: In situ temperature gradient measurements (red) compared to what a strictly linear temperature gradient would look like (blue) after steady state heat flow was achieved in a laboratory prepared ice-snow specimen with a 4 mm ice lens. Adapted from Hammonds et al. 2015 with permission from Elsevier and Cold Regions Science and Technology.

Upon incrementally turning down the temperature gradient in this experiment from $-100^{\circ}\text{C m}^{-1}$ to $-50^{\circ}\text{C m}^{-1}$, $-10^{\circ}\text{C m}^{-1}$, and $-4^{\circ}\text{C m}^{-1}$, it was found that an inverse exponential relationship exists between the imposed and measured temperature gradients. We describe this apparent phenomenon by taking the ratio, termed the Temperature Gradient Multiplier (TGM), of the observed to the imposed temperature gradient, given in Eq. (1).

$$TGM = \frac{\text{Observed Temperature Gradient}}{\text{Imposed Temperature Gradient}} \quad (1)$$

From this experiment, the TGM is plotted in Fig. 4 as a function of the imposed bulk temperature

gradient. The utility of taking the TGM is that it shows that as the imposed bulk temperature gradient is decreased, the degree to which the local temperature gradient is greater than the imposed bulk temperature gradient increases inversely. This would indicate that even at very low ($\leq -10^{\circ}\text{C m}^{-1}$) bulk measured temperature gradients, the local temperature gradient at an ice-snow interface may be many times greater than would have been previously thought via a more conventional continuum approach.

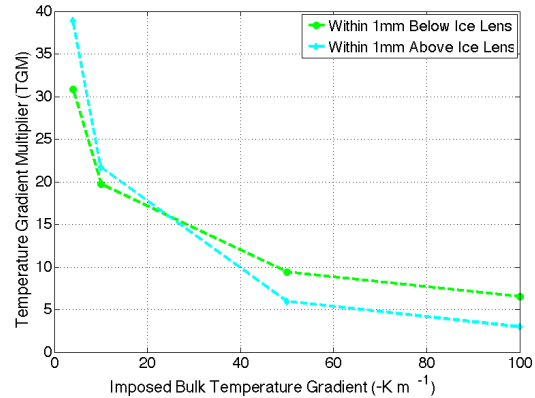


Fig. 4: TGM plotted as a function of the imposed bulk temperature gradient, illustrating an inverse relationship. Adapted from Hammonds et al. 2015 with permission from Elsevier and Cold Regions Science and Technology.

In a separate set of experiments, X-ray computed micro-tomography was used to capture time-lapse images of the microstructural evolution of the ice-snow interface in our ice-snow specimens while under a constant temperature gradient. From this analysis, in addition to showing evidence of new ice crystal growth occurring from the bottom (warmer) surface of the ice lens, some interesting trends in the local porosity near the ice-snow interface were observed as well. In our calculations of the porosity, shown in Fig. 5, we looked at four different regions above and below the ice lens. These regions were defined by the tracking of the region of new ice crystal growth below the ice lens, a 0.3 mm space above the ice lens, and the regions of bulk snow grains above and below the ice lens. Just below the ice lens, a relatively high initial porosity of around 70-80% was observed, followed by a steady decrease and stabilization near 60% porosity. When compared to the remainder of the snow grains below this region of new ice crystal growth, which remained steady at 50-55% porosity, this value is approximately 5-10% larger on average. Directly above the ice lens, the 0.3 mm region remained stable over time

near 55-60%, but it was typically 5% greater than that for the region for the snow grains above the ice lens and 5% less than the porosity of the region of new ice crystal growth directly below the ice lens. It is thought that these differences in the porosity near the ice-snow interface could have a significant effect on the observed temperature gradient, as higher values in the porosity below the ice lens would imply fewer connections between the snow grain structure and the ice lens.

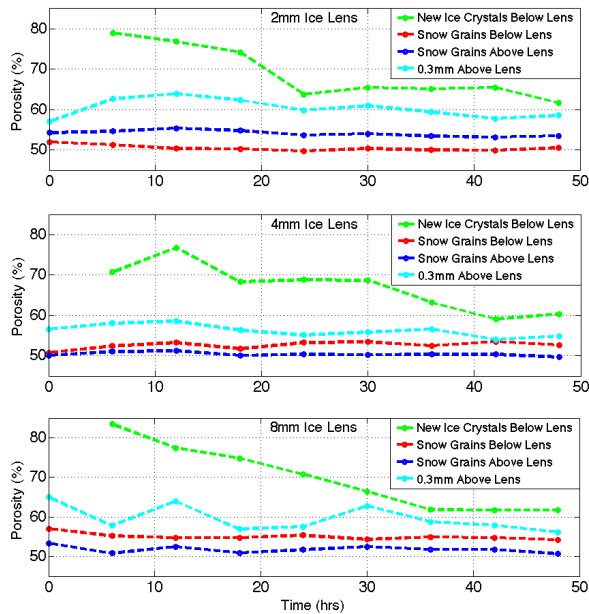


Fig. 5: Porosity for the 2 mm, 4 mm, and 8 mm ice lens cases, while under an imposed temperature gradient of -100 K m^{-1} . Adapted from Hammonds et al. 2015 with permission from Elsevier and Cold Regions Science and Technology.

2.2 Conductive heat flow

In a porous medium, such as snow, the temperature gradient through the material is controlled by the effective thermal conductivity, which accounts for the combination of the thermal conductivities of the solid (ice) and fluid (air) that fills the pore space (Bergman et al. 2011). From Riche & Schneebeli 2013, for snow of a similar shape, density, and SSA, we estimate the thermal conductivity of our snow sample to be near $0.219 \text{ W m}^{-1} \text{ K}^{-1}$ (see their Table 1 in Supplementary Material, snow type: RGsr). This value is roughly a full order of magnitude greater than that of dry air ($k_{air} = 0.024 \text{ W m}^{-1} \text{ K}^{-1}$ at 273 K, Wallace & Hobbs 2006) and a full order of magnitude less than that of pure polycrystalline ice ($k_{ice} = 2.4 \text{ W m}^{-1} \text{ K}^{-1}$ at 253 K, Petrenko & Whitworth 1999). Such a discontinuity in thermal conductivities at the ice-snow

interface would suggest the possibility of thermal contact resistance as a contributing mechanism to the observed temperature drop, as illustrated in Fig. 6 (adapted from Cengel 2007, see his Figure 3-14).

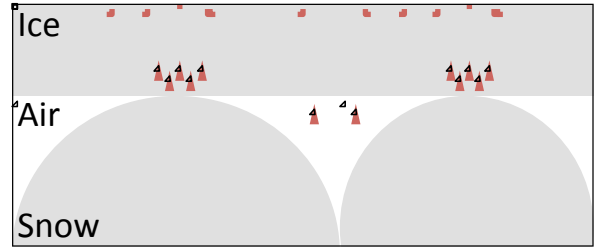


Fig. 6: Idealized representation of the conductive heat flow at the interface between a solid layer of ice and a porous layer of snow. Adapted from Hammonds et al. 2015 with permission from Elsevier and Cold Regions Science and Technology.

As shown in this idealized representation, the conductive heat flow is ultimately limited by the number of connections that can exist between the snow and ice, which is itself limited by the size and shape of the snow grains, the roughness of the ice lens, and the porosity of the bulk snowpack at the interface. As the connectivity increases, the effective thermal conductivity also increases, which would then decrease the temperature gradient if conduction were the only heat transfer mechanism. Notice in Fig. 3, that it is highest thermal conductivity material (ice) that also has the smallest temperature gradient and in Fig. 5, the initial porosity below the ice lens was much greater than that of the bulk, but decreased over time. A decrease in the porosity at the interface could be perceived as analogous to an increase in the connectivity, which supports the observations of ice crystal growth from the bottom side of the ice lens, but does not further elaborate on the factor of two difference in the temperature gradient above the ice lens as compared to below. In contemplating this difference, all possible mechanisms of heat flow must be considered.

2.3 Thermal contact resistance

When performing heat and mass transfer calculations between two solids, it is common to assume perfect contact between the two, and thus no temperature drop at their interface (Cengel 2007). In reality, even machined surfaces that appear to be smooth are only making contact at a very limited number of spots and the remainder of space is

typically filled with air (Kakac & Yener 1993). Due to the thermal conductivities of most solids being much greater than that of air, heat flow paths are forced to converge toward the actual points of contact. As described earlier, the effective thermal conductivity is a function of the porosity of the medium. At the interface between a porous material and a solid, however, the question becomes “To what degree is the temperature gradient at the interface influenced by the porosity of the medium and thereby the effective thermal conductivity vs. the conductive connectivity between the two materials?” For the ice-snow interface, the phenomenological representation of such a conductive connectivity limitation, termed the thermal contact resistance (Kakac & Yener 1993), was first illustrated in Fig. 6.

A brief review of current literature shows that only recently have heat and mass transfer studies begun to look more closely at the problem of interfacial influences causing large temperature gradients between porous and solid materials, namely in the joining of porous aluminum alloy foams to solid iron surfaces (Sadeghi et al. 2011). In Sadeghi et al. 2011, the authors suggest that “the fundamental issue with combining the two [thermal contact resistance and effective thermal conductivity] is that the thermal contact resistance is an *interfacial phenomenon* which is a function of mechanical load, surface characteristics and thermal conductivity of both interfacing surfaces, whereas thermal conductivity is a transport coefficient characterizing the *bulk medium*.” In other words, combining the effects of thermal contact resistance with the effective thermal conductivity is not sufficient in understanding heat flow through a porous-solid interface. In their conclusions, Sadeghi et al. 2011 ultimately cite from their experimental results that the phenomenon of thermal contact resistance had accounted for more than 50% of the total thermal resistance and temperature drop observed at their porous-solid interface.

3. METHODS

As first described in Part I of this study, our in situ temperature gradient measurements were made using a micro-thermocouple array that had been integrated into the polycarbonate tube that acted as the housing for our ice-snow specimen. We recorded a total of 12 in situ temperature measurements with 4 micro-thermocouples placed within 1 mm above and below the ice lens and 2 additional micro-thermocouples at distances of 8 and 16 mm away from the ice lens. To facilitate our thermodynamic analysis, the topic of Part II,

we segregated our temperature gradient measurements into five distinct regions, R_1 , R_2 , R_3 , R_4 , and R_{ice} . These segments correlate to the five unique temperature gradients we observed over the height of our specimen under conditions of steady state heat flow and a 24 hour recording period. The imposed temperature gradient for this 24 hour recording period was held at $-100^\circ\text{C m}^{-1}$. The location of each of these regions is illustrated schematically in Fig. 7, which has been adapted from Fig. 3.

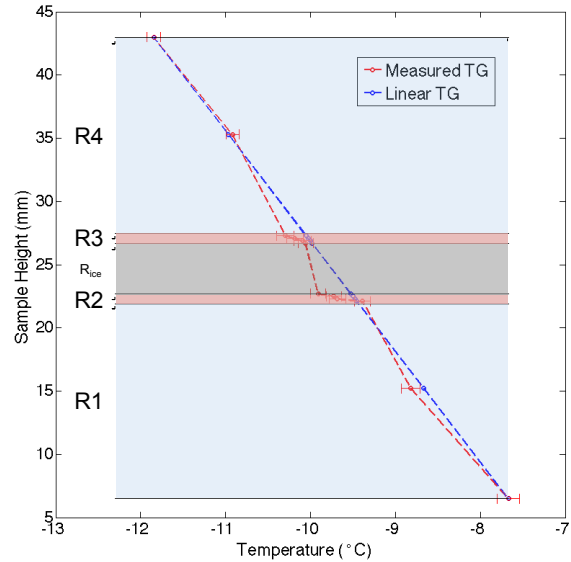


Fig. 7: Regions (R_1 , R_2 , R_{ice} , R_3 , R_4) identified for 1-D in situ micro-thermocouple analysis. Adapted from Hammonds & Baker 2016 with permission from Elsevier and Cold Regions Science and Technology.

It should be noted that because the location of the micro-thermocouples was not precisely known above and below the ice lens, all calculations for the temperature gradient in these regions (R_2 and R_3) are for a ΔZ of 0.8 mm, and in the analysis given here, we have allowed ΔZ to vary from 0.6 mm to 1 mm in order to provide a conservative range for all calculations. This variability is incorporated into the analysis in the form of box and whiskers plots that has been overlaid on top of all bar plots given to display our quantitative results.

In order to satisfy the requirements for an energy balance in our 1-D energy balance model, we assume that the total heat flux Q_{tot} (W m^{-2}), as given in Eq. (2), at the interface of each region must be equal to the total heat flux of the adjacent interface (i.e. $Q_{R1} = Q_{R2} = Q_{R_{ice}} = Q_{R3} = Q_{R4}$).

$$Q_{tot} = q_{latent\ heat} + q_{conduction} \quad (2)$$

We then allow the effective thermal conductivity to vary within R_1 - R_4 according to our temperature gradient measurements and our requirements for energy balance. Utilizing this approach, we can then estimate the relative contributions for $q_{latent\ heat}$ and $q_{conduction}$ towards Q_{tot} in each region. In establishing a fixed Q_{tot} , for which the energy balance must be accommodated, we use the temperature measurements from directly above and below the ice lens. We see this as the most reliable measure of Q_{tot} because 1) our ice lenses were made from pure polycrystalline ice, suggesting that pure conduction would be the only heat flow mechanism possible in R_{ice} , and 2) the thermal conductivity of polycrystalline ice is well known. Based on this energy balance requirement, we then expect that Q_{R1} - Q_{R4} must be equal to $Q_{R_{ice}}$.

4. RESULTS & ANALYSIS

Given in this section are the results from our comparative analysis on all the mechanisms thought possible for heat and mass transfer in our experiments that include

- i. Thermal contact resistance.
- ii. Increases in the porosity and decreases in the effective thermal conductivity.
- iii. Latent heating/cooling.
- iv. Normal contribution from an imposed linear temperature gradient.

The goal of this analysis was to ultimately identify which of these mechanisms was primarily responsible for the observed enhancement in the temperature gradient near the ice-snow interface in our experiments. For brevity, only the general results from this analysis are given here, which are best summarized in Figs. 8 and 9 but the reader is referred to Hammonds & Baker (2016) for additional details and explanations. As can be seen in these figures, it was found that thermal contact resistance was the primary contributor to the enhancement of the temperature gradient both above and below the ice lens. This was somewhat of a surprising result, as latent heat release was originally expected to be a larger contributor to the observed temperature gradient.

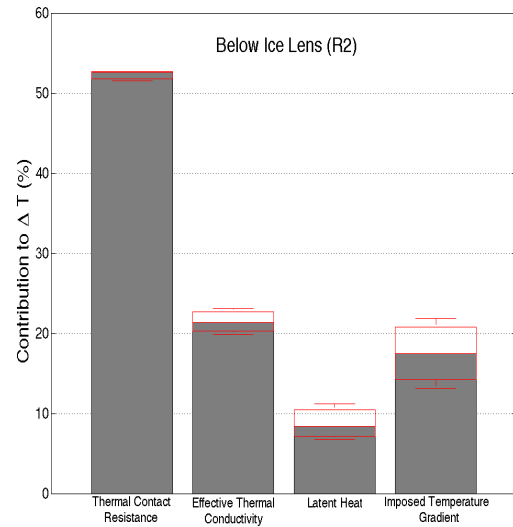


Fig. 8: Contributions to the temperature gradient (ΔT) observed below the ice lens in R_2 by mechanism. Adapted from Hammonds & Baker 2016 with permission from Elsevier and Cold Regions Science and Technology.

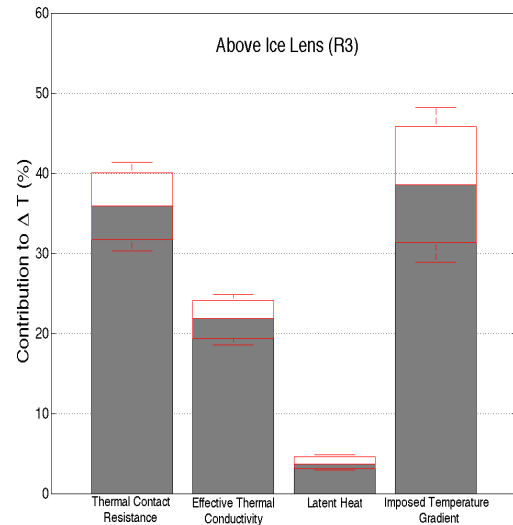


Fig. 9: Contributions to the temperature gradient (ΔT) observed above the ice lens in R_2 by mechanism. Adapted from Hammonds & Baker 2016 with permission from Elsevier and Cold Regions Science and Technology.

5. DISCUSSION & CONCLUSIONS

In some respects, the results shown in Figs. 8 and 9 should not be too surprising. If considering the packing of monodisperse solid spherical particles

as an analog to the packing of snow grains near a similarly flat interface, it has been observed that the packing efficiency increases in the layers nearest the interface and that the porosity in turn is decreased (Nesterenko 2001). This phenomenon occurs due to the interface creating order in the packing of the particles in contact with the interface, whereas further away, as more particles are added to the matrix, they become more randomly placed and packed, as illustrated in Fig. 10 (adapted from Nestrenko 2001, Fig. 2.33).

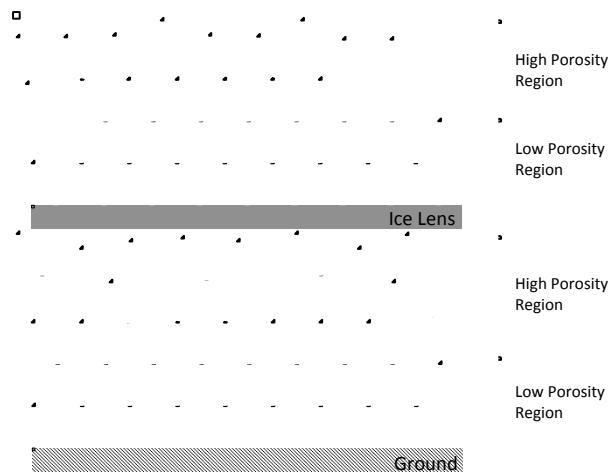


Fig. 10. Idealized representation of snow grains as a collection of monodisperse spherical particles. Packing efficiencies are increased above solid flat interfaces. Adapted from Hammonds & Baker 2016 with permission from Elsevier and Cold Regions Science and Technology.

In this idealized representation, the effects of the ice lens could be interpreted to increase the porosity of the monolayer below the ice lens while decreasing the porosity above the ice lens, which is consistent with what we observed in our time-lapse μ -CT experiments (see Fig. 5). Below the ice lens, this effect would act to increase the thermal contact resistance at the interface while decreasing the effective thermal conductivity. Above the ice lens, the more efficiently packed monolayer would act to decrease thermal contact resistance and increase the effective thermal conductivity in this region. Such an interpretation would also be consistent with the difference in the temperature gradients observed above and below the ice lens, as shown in Fig. 3. Also of note, are the effects of compression on these layers, as it has been shown in other materials that upon increasing the unidirectional pressure in the z-direction (as shown in Fig. 10) the thermal contact resistance

should decrease (Sadeghi et al. 2011). For the case of natural snowpacks, this introduces the idea of whether or not the ice lens or perhaps some other icy layer or crust may be able to act as a “bridge” over the adjacent layer of snow directly below the ice lens (Jones et al. 2006). If so, new ice crystal growth in this region would then be the primary mechanism for increasing the effective thermal conductivity while decreasing the thermal contact resistance. In either instance, the latent heat flux driven by diffusion and deposition/sublimation would be expected to remain fairly constant, but appears to be of only minor significance to the magnitude of the measured temperature gradient.

If considering our laboratory specimen as analogous to a natural snowpack, our findings would indicate that the porosity of the snowpack just near the ice-snow interface would be of primary importance to kinetic snow metamorphism and subsequent weak layer development in this region based on enhancements in the local temperature gradient. For field practitioners, these results suggest that although obtaining a measurement of the thermal contact resistance would be difficult, obtaining porosity measurements as an inverse analog to thermal contact resistance could be useful and attainable via hand-hardness or density measurements. We point out, however, that in our experiments we have only studied the effects of coarsened snow grains and lenses of artificially created polycrystalline ice.

In future work, we recommend that similar experiments be performed for additional temperature gradients, a variety of snow grain types, and an assortment of naturally collected ice lenses and crusts. This approach would be very similar to what was originally attempted in Greene 2007. Additional mechanical testing of these layers would also be useful in further understanding the effects of temperature gradients and microstructures on mechanical failure.

ACKNOWLEDGEMENTS

This work was supported by the American Avalanche Association Theo Meiners research grant and the National Science Foundation grant number PLR 1141411. The authors acknowledge the use of the Ice Research Laboratory (Director E.M. Schulson) at the Thayer School of Engineering at Dartmouth College. The authors also thank Dr. Niede Calonne for her thoughtful comments and insight during the review process for Part II of this work.

REFERENCES

- Adams, E.E., and R.L. Brown, 1990: A mixture theory for evaluation heat and mass transport processes in nonhomogeneous snow. *Continuum Mechanics and Thermodynamics*, 2, 31-63.
- Bergman, T.L., Lavine, A.S., Incropera, F.P., and D.P. Dewitt, 2011: *Fundamentals of Heat and Mass Transfer*. John Wiley and Sons, 1048 pp.
- Calonne, N., Flin, F., Geindreau, C., Lesaffre, B., and S. Rolland du Roscoat, 2014: Study of a temperature gradient metamorphism of snow from 3-D images: time evolution of microstructures, physical properties and their associated anisotropy. *The Cryosphere*, 8, 2255-2274.
- Cengel, Y.A., 2007: *Heat and Mass Transfer: A Practical Approach*, Third Edition, McGraw Hill, 901 pp.
- Chen, S., and I. Baker, 2010: Structural evolution during ice-sphere sintering. *Hydrological Processes*, 24, 2034-2040.
- Colbeck, S.C., 1991: The layered character of snow covers. *Reviews of Geophysics*, 29, 81-96.
- Colbeck, S.C., and J.B. Jamieson, 2001: The formation of faceted layers above crusts. *Cold Regions Science and Technology*, 33, 247-252.
- Flin, F., and J.B. Brzoska, 2008: The temperature-gradient metamorphism of snow: vapour diffusion model and application to tomographic images, *Annals of Glaciology*, 49(1), 17-21.
- Greene, E.M., 2007: The thermophysical and microstructural effects of an artificial ice layer in natural snow under kinetic growth metamorphism. *Ph.D. Dissertation*, Colorado State University, 147 pp.
- Hammonds, K.H., Lieb-Lappen, R., Baker, I., and X. Wang, 2015: Investigating the thermophysical properties of the ice-snow interface under a controlled temperature gradient – Part I: Experiments and Observations. *Cold Regions Science and Technology*, 120, 157-167.
- Hammonds, K.H., and I. Baker, 2016: Investigating the thermophysical properties of the ice-snow interface under a controlled temperature gradient – Part II: Analysis. *Cold Regions Science and Technology*, 125, 12-20.
- Jones, A.S.T., Jamieson, J.B., and J. Schweizer, 2006: The effect of slab and bed surface stiffness on the skier-induced shear stress in weak snow cover layers. In: Gleason, J.A. (Ed.), *Proceedings of the International Snow Science Workshop 2006*, Telluride CO, U.S.A., 1–6 October 2006, p. 157-164.
- Kakac, S. and Y. Yener, 1993: *Heat Conduction*. Taylor & Francis, 363 pp.
- Nesterenko, V.F., 2001: *Dynamics of Heterogeneous Materials*. Springer, NY, 528 pp.
- Petrenko, V.F. and W. Whitworth, 1999: *Physics of Ice*. Oxford University Press, 373 pp.
- Pinzer, B., Schneebeli, M., and T. Kaempfer, 2012: Vapor flux and recrystallization during dry snow metamorphism under a steady temperature gradient as observed by time-lapse micro-tomography, *The Cryosphere*, 6(3), 1673-1714.
- Riche, F. and M. Schneebeli, 2013: Thermal conductivity of snow measured by three independent methods and anisotropy considerations. *The Cryosphere*, 7, 217-227.
- Sadeghi, E., Hsieh, S., and M. Bahrami, 2011: Thermal conductivity and contact resistance of metal foams. *J. Phys. D: Appl. Phys.* 44, 125406.
- Wallace, J.M., and P.V. Hobbs, 2006: *Atmospheric Science: An Introductory Survey*. Elsevier, 483 pp.